

## EFFECT OF GADOLINIUM SUBSTITUTION ON MAGNETOCALORIC PROPERTIES OF LANTHANUM STRONTIUM MANGANITES

S. PHROMCHUAI<sup>a</sup>, C. SIRISATHITKUL<sup>b\*</sup>, P. JANTARATANA<sup>a</sup>

<sup>a</sup>*Department of Physics, Faculty of Science, Kasetsart University, Bangkok, Thailand*

<sup>b</sup>*Magnet Laboratory, School of Science, Walailak University, Nakhon Si Thammarat, Thailand*

Magnetocaloric effect in sol-gel derived  $\text{La}_{0.75-x}\text{Gd}_x\text{Sr}_{0.25}\text{MnO}_3$  was studied as a function of temperature and magnetic field. The crystallite size of the rhombohedral manganites was increased and the magnetisation was decreased with increasing Gd doping from  $x = 0-0.3$ . By using the indirect measurement, the entropy change computed from temperature-dependent magnetisation was proportional to the applied DC magnetic field. Under the field of 0.7 T, the maximum entropy changes of 0.93-1.14 J/kg·K were observed around the Curie temperature ( $T_C$ ) determined by AC magnetic susceptometry. The  $T_C$  was decreased with the increase in  $x$ . The maximum magnetocaloric effect occurred in the sample with  $x = 0.15$  and it could be used in magnetic refrigeration near the room temperature.

(Received December 13, 2013; Accepted February 12, 2014)

*Keywords:* Magnetocaloric effect, Sol-gel synthesis, Lanthanum strontium manganites, Gadolinium

### 1. Introduction

Lanthanum manganite perovskites ( $\text{LaMnO}_3$ ) can be implemented as catalytic and piezoelectric materials [1]. Furthermore, doped  $\text{La}_{1-x}\text{A}_x\text{MnO}_3$  (A are divalent metallic ions) such as  $\text{La}_{1-x}\text{Ca}_x\text{MnO}_3$  and  $\text{La}_{1-x}\text{Ca}_x\text{MnO}_3$  exhibit several interesting phenomena including metal-insulation transition, colossal magnetoresistance and magnetocaloric effect [2, 3]. Magnetocaloric effect is the entropy change in response to an externally applied magnetic field as a result of transitions in the lattice structure during the magnetisation process [4, 5]. Magnetic refrigerators can be developed by exploiting the large change in temperature around the magnetic-ordering phase transition. The ferromagnetic-paramagnetic transition occurs at the Curie temperature ( $T_C$ ). Since the properties of manganites are modified by the doping process, this  $T_C$  as well as other parameters could be tailored. Gadolinium (Gd) is a logical selection as a dopant due to its manifestation of magnetocaloric effect at room temperature. While the  $T_C$  were both decreased by Gd substitutions of La, the magnetocaloric effect was increased in  $\text{La}_{0.67-x}\text{Gd}_x\text{Ca}_{0.33}\text{MnO}_3$  [6] but decreased in  $\text{La}_{0.5-x}\text{Gd}_x\text{Ca}_{0.5}\text{MnO}_3$  [7]. For  $\text{La}_{0.67-x}\text{Gd}_x\text{Sr}_{0.33}\text{MnO}_3$ , the  $T_C$  is reduced from 358 to 270 K with increasing Gd substitution [8-11]. By applying very large magnetic field of 8 T, the entropy change in such systems can be as high as 8.8 J/kg·K [8].

In addition to the solid state reaction, the sol-gel technique can be used to synthesize manganites [9-12]. The advantages are the lower processing temperature for sol-gel derived products and the tendency to obtain higher  $T_C$  [11]. This work is aimed to explore the variation in magnetocaloric properties of sol-gel derived  $\text{La}_{0.75-x}\text{Gd}_x\text{Sr}_{0.25}\text{MnO}_3$  with several doping concentrations. By understanding the influence on the properties, the advantage of Gd substitutions could be highlighted to fully realise the potential applications of these magnetocaloric materials.

---

\*Corresponding author: chitnarong.siri@gmail.com

## 2. Experimental

Seven  $\text{La}_{0.75-x}\text{Gd}_x\text{Sr}_{0.25}\text{MnO}_3$  samples with  $x = 0, 0.05, 0.10, 0.15, 0.20, 0.25$  and  $0.30$  were prepared by the sol-gel technique. Gadolinium nitrate hexahydrate ( $\text{Gd}(\text{NO}_3)_3 \cdot 6\text{H}_2\text{O}$ , 99.9%), lanthanum nitrate hexahydrate ( $\text{La}(\text{NO}_3)_3 \cdot 6\text{H}_2\text{O}$ , 99.999%), manganese nitrate hydrate ( $\text{Mn}(\text{NO}_3)_2 \cdot x\text{H}_2\text{O}$ , 99.99%), strontium nitrate ( $\text{Sr}(\text{NO}_3)_2$ , 99.995%), citric acid ( $\text{C}_6\text{H}_8\text{O}_7$ ), polyethylene glycol were all purchased from Aldrich. All nitrates were firstly dissolved in distilled water. After mixing with the citric acid solution, the solution was stirred on a hot plate with a magnetic stirrer for about 50 min. Polyethylene glycol was then added and the solution gradually turned into gel. The gel was allowed to cool down, dried at 383 K for 12 h, heated at 523 K for 5 h and fired at 1073 K for 5 h (heating rate 5 K/min and cooling rate 3 K/min). The products were ground and pressed into pellets under the pressure of 4.9 MPa for 15 min. Finally, the pellets were fired at 1473 K for 10 h (heating rate 5 K/min and cooling rate 2 K/min).

Structures of the products were characterised by x-ray diffraction (XRD) using  $\text{Cu-K}_\alpha$  radiation. Magnetic properties were studied by AC susceptometry and vibrating sample magnetometry (VSM). To measure magnetic susceptibility ( $\chi$ ), each pellet was installed at the end of sample probe whose temperature was reduced under zero applied DC magnetic field ( $H_{\text{DC}}$ ). Under the 20 Oe  $H_{\text{DC}}$  and the 10 Oe AC magnetic field ( $H_{\text{AC}}$ ) at 999 Hz, the real part of susceptibility ( $\chi'$ ) was recorded as a function of the temperature from 120 to 324 K (rate 2 K/min).  $d\chi/dT$  was also plotted against the temperature to determine the  $T_C$ . In the VSM measurement, each pellet was installed in the temperature-control tube. The heating/cooling source of the tube was connected to the pump. In addition to hysteresis tracing at room temperature, the magnetisation was measured at temperatures 264-360 K with 6 K interval as a function of magnetic field up to 0.7 T. In the indirect measurement of magnetocaloric effect, the entropy change  $|\Delta S_M|$  was calculated from the measured magnetisation according to the following equation:

$$|\Delta S_M| \approx \sum_i \frac{M_i - M_{i+1}}{T_{i+1} - T_i} \Delta H$$

where  $M_i$  and  $M_{i+1}$  is the magnetization at temperature  $T_i$  and  $T_{i+1}$  respectively.  $\Delta H$  is the difference of magnetic field.

## 3. Results and discussion

All XRD patterns in *Fig. 1* show characteristic peaks of the rhombohedral perovskite structure with the space group R-3C (JCPDS No. 89-8093). The intensity of the peak is monotonically increased with increasing  $x$ . The substitution of Gd apparently increases the crystallite size. For all Gd doping concentrations, the  $\chi'$  in *Fig. 2a* is rather insensitive to the increase in temperature up to a certain temperature. Beyond this temperature, the  $\chi'$  abruptly drops signifying the ferromagnetic-paramagnetic transition. The  $T_C$  can be experimentally deduced by plotting  $d\chi/dT$  curves in *Fig. 2b* and identifying their peaks. The increase in  $x$  from 0.1 to 0.3 reduces the  $T_C$  which can be explained in terms of the reduction in average ionic radius [8-11]. For  $x = 0$  and 0.05, the peak is out of the measurement range and their  $T_C$  cannot be concluded.

From magnetisation curves at 300 K shown in *Fig. 3a*, the substitution of Gd for La can clearly be divided into 4 ranges, i.e.  $x = 0-0.10$ ,  $0.15-0.20$  and  $0.25-0.30$ . In addition to minimal magnetisation in the case of  $x = 0.25$  and  $0.30$ , the paramagnetic behaviour is observed with a linear variation in magnetisation at room temperature. For ferromagnetic manganites with  $x = 0-0.20$ , the coercive field is determined from the x-intercept of the magnetisation curves whereas the y-intercept corresponds to the remanent magnetization. These magnetic parameters are summarised in Table 1. For  $x = 0-0.20$ , the coercive field deduced from ferromagnetic behaviours is clearly decreased. Commonly, the reduction in coercive field has a positive effect on magnetocaloric effect [5]. As shown in Table 1, the substitution of Gd also reduces the maximum and remanent magnetisations. By virtue of thermal agitations, all magnetisations are decreased

with the increase in temperature from 264 to 360 K as exemplified in the case of  $x = 0.15$  in Fig. 3b.

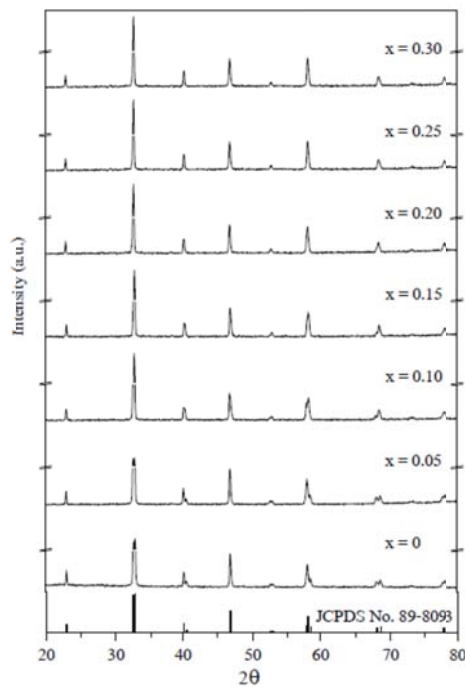
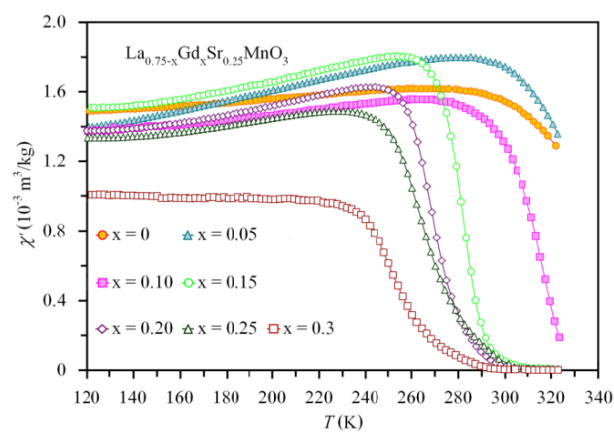
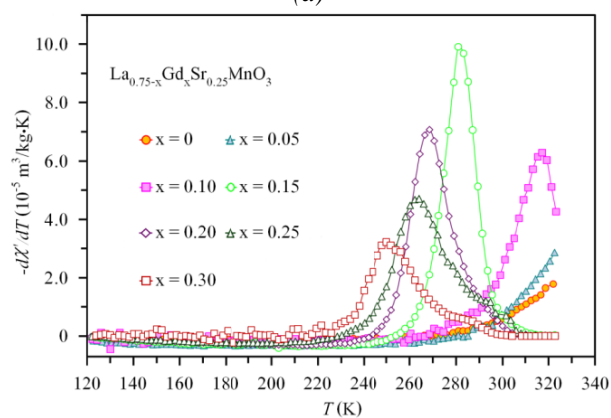


Fig. 1. XRD patterns of  $\text{La}_{0.75-x}\text{Gd}_x\text{Sr}_{0.25}\text{MnO}_3$  for  $x = 0-0.30$  compared with reference standard.



(a)



(b)

Fig. 2. (a) real part of susceptibility ( $\chi$ ) and (b)  $d\chi/dT$  measured in  $\text{La}_{0.75-x}\text{Gd}_x\text{Sr}_{0.25}\text{MnO}_3$  for  $x = 0-0.30$  as a function of temperature from 120 to 324 K.

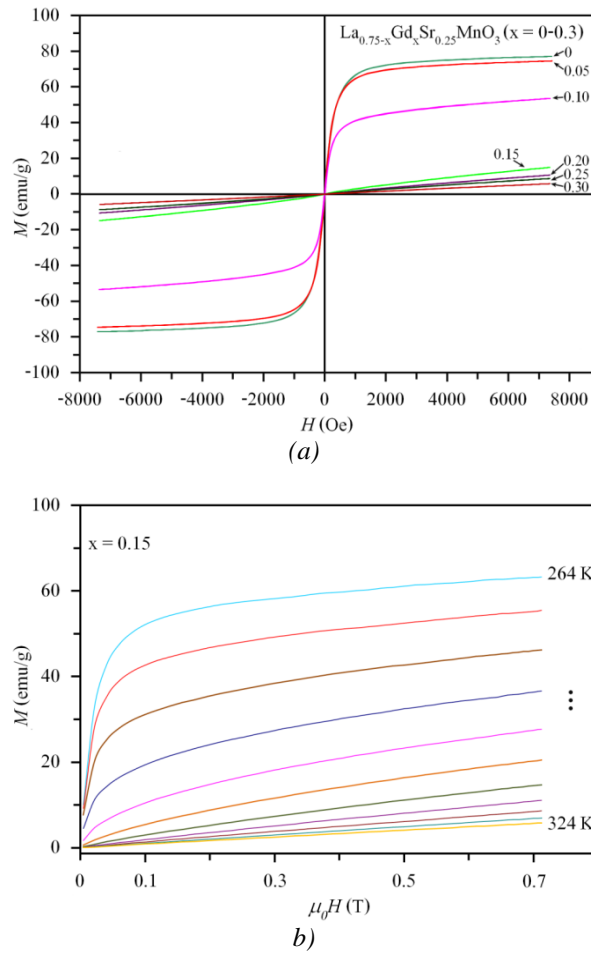


Fig. 3. Magnetisation curves of  $\text{La}_{0.75-x}\text{Gd}_x\text{Sr}_{0.25}\text{MnO}_3$  (a) for  $x = 0-0.30$  at room temperature and (b) for  $x = 0.15$  at 264-324 K.

Table 1 Variations in magnetic parameters, the Curie temperature ( $T_C$ ) measured by AC susceptibility and the temperature ( $T_{max}$ ) at which the maximum entropy change occurs ( $|\Delta S_{max}|$ ) with Gd substitution ( $x$ ) in  $\text{La}_{0.75-x}\text{Gd}_x\text{Sr}_{0.25}\text{MnO}_3$ .

x	Maximum magnetisation (emu/g)	Remanent magnetisation (emu/g)	Coercive field (Oe)	$T_C$ (K)	$T_{max}$ (K)	$ \Delta S_{max} $ (J/kg·K)
0	77.19	2.440	11.3	-	339	0.93
0.05	74.71	1.850	8.6	-	333	1.03
0.10	53.57	1.230	7.4	317	309	1.09
0.15	14.95	0.034	7.2	281	279	1.14
0.20	10.64	0.005	2.0	267	-	-
0.25	8.77	-	-	264	-	-
0.30	5.81	-	-	250	-	-

The entropy changes ( $|\Delta S_M|$ ) computed from the change in magnetisation at varying temperature are plotted against the temperatures at 264-360 K in Fig. 4a. In this temperature range, the  $|\Delta S_M|$  is maximised at 1.14 J/kg·K in the case of  $x = 0.15$ . However, the temperature at which the maximum effect occurs ( $T_{max}$ ) is reduced with increasing  $x$  and the peaks in the case of  $x = 0.2-0.3$  are not observed in this temperature range. For  $x = 0.10$  and  $0.15$ ,  $T_{max}$  from magnetisation and  $T_C$  from susceptibility measurements were comparable. This agrees with

previous experiments that the entropy change reached the maximum around the  $T_C$  [4, 5]. Regardless of the  $T_C$ , the entropy change at 300 K for each Gd doping concentration is higher than that of  $\text{La}_{0.75}\text{Sr}_{0.25}\text{MnO}_3$  and this enhanced magnetocaloric effect under the modest magnetic field can be implemented around the room temperature.

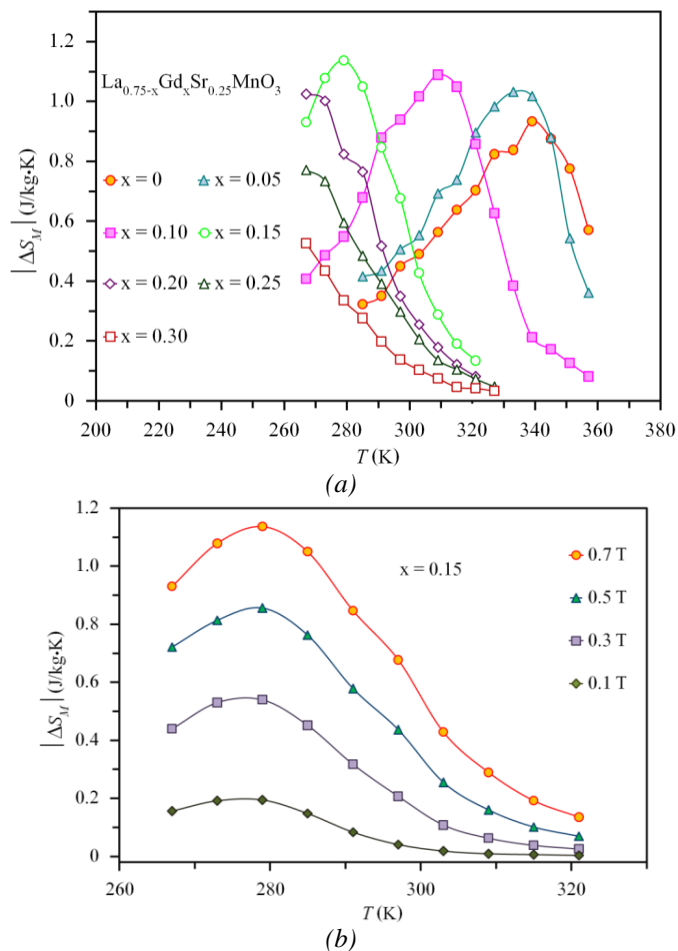


Fig. 4. Temperature-dependent entropy changes ( $|\Delta S_{max}|$ ) of  $\text{La}_{0.75-x}\text{Gd}_x\text{Sr}_{0.25}\text{MnO}_3$  (a) for  $x = 0-0.30$  under 0.7 T magnetic field and (b) for  $x = 0.15$  under 0.1-0.7 T magnetic field.

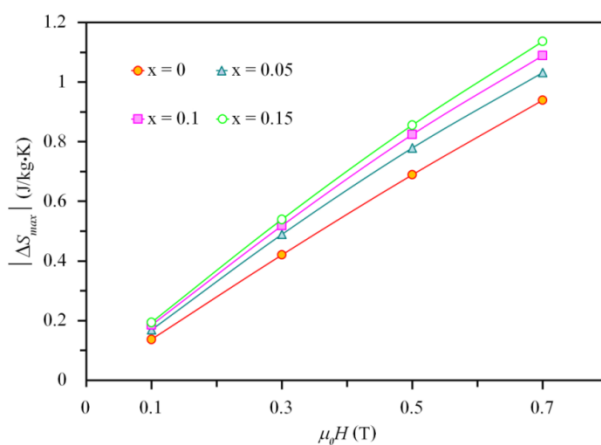


Fig. 5. Maximum entropy changes ( $\Delta S_{max}$ ) measured in  $\text{La}_{0.75-x}\text{Gd}_x\text{Sr}_{0.25}\text{MnO}_3$  for  $x = 0-0.15$  as a function of magnetic field ( $\mu_0 H$ ) from 0.1 to 0.7 T.

The  $|\Delta S_M|$  is further studied as a function of applied  $H_{DC}$  in *Fig. 4b*. The effect at 264-360 K is predictably increased with the increase in  $H_{DC}$  from 0.1 to 0.7 T. Finally, the maximum entropy changes ( $|\Delta S_{max}|$ ) are determined from the peaks in *Fig. 4b* and plotted as a function of  $H_{DC}$  in *Fig. 5*. The  $|\Delta S_{max}|$  is directly proportional to magnetic field. The linear variation is also obtained in the case of  $x = 0, 0.05$  and  $0.10$  as seen in the other plots in *Fig. 5*. This linear trend was also observed in  $La_{0.5}Gd_{0.2}Sr_{0.3}MnO_3$  [8].

#### 4. Conclusion

$La_{0.75-x}Gd_xSr_{0.25}MnO_3$  samples prepared by the sol-gel technique exhibit decreases in magnetisation, coercive field and  $T_C$  with increasing Gd substitution from  $x = 0$  to  $0.30$ . Above all, the substitution of Gd for La enhances the magnetic entropy change in  $La_{0.75}Sr_{0.25}MnO_3$  around room temperature. From the measurement at 264-324 K,  $x = 0.15$  maximises the entropy change and such change has a linear variation with magnetic field from 0.1 to 0.7 T.

#### Acknowledgements

This work was funded by Faculty of Science, Kasetsart University. The authors would like to thank Scientific Equipments Center, Kasetsart University for the XRD characterisation.

#### References

- [1] N. Razlescu, E. Razlescu, C. Doroftei, P. D. Popa, M. Ignat, *Dig. J. Nanomat. Biostruct.* **8**, 581 (2013).
- [2] M. Pekala, K. Pekala, V. Drozd, J. F. Fagnard, P. Vanderbemden, *J. Magn. Magn. Mater.* **322**, 3460 (2010).
- [3] C. I. Covaliu, T. Malaer, G. Georgescu, O. Oprea, L. Alexandrescu, I. Jitaru, *Dig. J. Nanomat. Biostruct.* **6**, 1491 (2011).
- [4] W. Zhong, C.-T. Au, Y.-W. Du, *Chin. Phys. B* **22**, 057501 (2013).
- [5] M.-H. Phan, S.-C Yu, *J. Magn. Magn. Mater.* **308**, 325 (2007).
- [6] H. Chen, C. Lin, D. Dai, *J. Magn. Magn. Mater.* **257**, 254(2003).
- [7] A. Krichene, W. Boujelben, A. Cheikhrouhou, *J. Alloys Compd.* **550**, 75 (2013).
- [8] Y. Sun, W. Tong, N. Liu, Y. Zhang, *J. Magn. Magn. Mater.* **238**, 25 (2002).
- [9] Z. Juan, W. Gui, *J. Magn. Magn. Mater.* **321**, 43 (2009).
- [10] Z. Juan, W. Gui, *J. Magn. Magn. Mater.* **321**, 2977 (2009).
- [11] G. Wang, Z. D. Wang, L. N. Zhang, *Mater. Sci. Eng. B.* **116**, 183 (2005).
- [12] M. H. Ensani, M. E. Ghazi, P. Kameli, *Dig. J. Nanomat. Biostruct.* **7**, 661 (2012).